ENG and NZRI Characteristics of Decagonal-Shaped Metamaterial for Wearable Applications

Kabir Hossain[1], Thennarasan Sabapathy[1*], Muzammil Jusoh[1], Ping Jack Soh[2], N. S. Raghava[3], Symon K. Podilchak[4], Dominique Schreurs[5], Qammer H. Abbasi[6]

[1]Bioelectromagnetics Research Group (BioEM), School of Computer and Communication Engineering, Universiti Malaysia Perlis, Arau 02600, Malaysia

[2]Advanced Communication Engineering (ACE) Centre of Excellence, School of Computer and Communication Engineering, Universiti Malaysia Perlis, 01000 Kangar, Perlis, Malaysia

[3]Departments of Electronics and Communication Engineering, Delhi Technological University, India

[4]Institute of Digital Communications, School of Engineering, University of Edinburgh, EH9 3FB, United Kingdom

[5]ESAT-TELEMIC Research Division, KU Leuven, Kasteelpark Arenberg 10 Box 2444, 3001 Leuven, Belgium

[6]School of Engineering, University of Glasgow, United Kingdom

[*]thennarasan@unimap.edu.my

***Abstract*—A decagonal-shaped split ring resonator metamaterial based on a wearable or textile-based material is presented in this work. Analysis and comparison of various structure sizes are compared considering a compact 6×6 mm^2 metamaterial unit cell, in particular, where robust transmission-reflection (RTR) and Nicolson-Ross-Weir (NRW) methods have been performed to extract the effective metamaterial parameters. An investigation based on the RTR method indicated an average bandwidth of 1.39 GHz with a near-zero refractive index (NZRI) and a 2.35 GHz bandwidth when considering epsilon negative (ENG) characteristics. On the other hand, for the NRW method, approximately 0.95 GHz of NZRI bandwidth and 2.46 GHz of ENG bandwidth have been observed, respectively. These results are also within the ultra-wideband (UWB) frequency range, suggesting that the proposed unit cell structure is suitable for textile UWB antennas, biomedical sensors, related wearable systems, and other wireless body area network communication systems.**

Keywords—metamaterial, near-zero refractive index (NZRI), negative-index metamaterial, epsilon negative (ENG).

I. INTRODUCTION

A new era of technological advancements has resulted in compact and intelligent biomedical sensors and antennas that can be worn on the human body. Moreover, Wireless Body Area Networks (WBAN) is a type of network that can employ these biosensors [1]. On-body wearable antennas have also attracted the attention of scholars globally due to their usefulness in applications for health monitoring, military, sports, and patient tracking [2][3][4], among others. More specifically for health monitoring applications, parameters such as blood pressure measurement, temperature measurement, Electroencephalogram (EEG) and the Electrocardiogram (ECG) can be monitored using WBAN [1].

Besides that, Ultrawideband (UWB) technology in WBANs can offer high bandwidth and operates within short-ranges using low power levels [2]. For on-body applications, antennas are ideally required to be compact in size, low profile and with satisfactory performance, especially catering to mobile users [5]. To ensure the safety and comfort of users, these antennas are best to be integrated into the clothing. The recent introduction of commercial conductive textiles has simplified the process of designing and implementing antennas for WBAN applications [6]. Nevertheless, the human body is of high permittivity, and antenna operation when spaced closely to the human body, must be accounted for in the design process [4], [7]. Integrating metamaterials (MTMs) into the antenna design may also mitigate coupling effectively, as proposed in [3], [8]. The promising feature of MTMs enables them to facilitate antenna enhancement in terms of gain and radiation patterns modification, besides improved size compactness and broadening of the operating bandwidth [9], [10].

MTMs are artificially created engineering materials that have electromagnetic properties which generally do not exist in nature. The characteristics of the MTM could be single negative (SNG) or double negative (DNG) based on the dielectric permittivity (ε) or, magnetic permeability (μ). If any are negative, it is known as SNG MTMs but for DNG MTM, both permittivity and permeability need to be negative [3], [11]. SNG metamaterials could be ε-negative (ENG) and\or μ -negative (MNG) materials. For the ENG materials, the permittivity is negative with positive permeability. In contrast, permeability is negative with positive permittivity for MNG materials [12]. Besides antenna designs, researchers have applied these unique properties of MTMs for different applications including wireless health monitoring [13], invisibility cloaking [14], bendable artificial magnetic conductors (AMC) [15], filters [16], sensors [17], and absorbers [18]. Furthermore, the refractive index of a material, which depends on the permittivity and permeability can decide the extent of reflection and refraction in a material [12]. The near-zero refractive index (NZRI) property can also enhance the gain as reported in [19]. Apart from that, an investigation on explicit applications based on NZRI, has shown improvement in antenna performance at S, C, and X bands [10]. MTMs of various forms have also been proposed, including complementary split-ring resonators (CSRR) [9], split-ring resonators (SRRs) [8], planar pattern and capacitance-loaded strips (CLSs) [11] as well as electromagnetic bandgap (EBG) structures [20].

Following these developments, a decagonal-shaped split ring resonator metamaterial with ENG and NZRI properties is proposed in this paper for wearable applications considering a textile-based material. Each unit cell is sized at 6×6 mm^2 and a different number of array configurations are studied; i.e. 1×1 , 2×1 , 1×2 and 2×2 unit cell configurations. Two methods are utilized to extract the effective parameters of each structure using the robust transmission-reflection (RTR) method [10], [21] and the Nicolson–Ross–Weir (NRW) method [22]. These results are then validated by a comparison between the two methods for all unit cell array configurations in terms of the ENG and the NZRI results. Based on this study, the average ENG bandwidth is about 2.35 GHz (6.89 GHz to 9.24 GHz) and the NZRI bandwidth is about 1.39 GHz (7.76

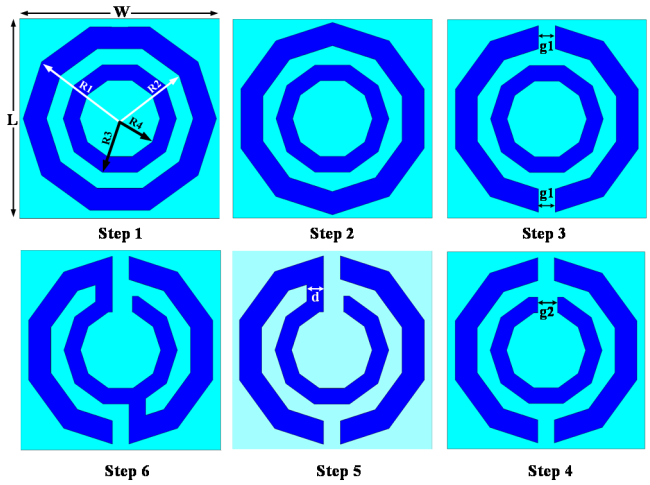

Fig. 1. Schematic and the evolution of the proposed unit cell.

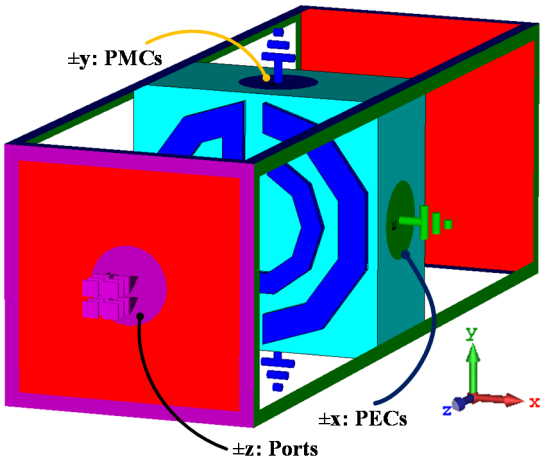

Fig. 2. 3D view of the simulation setup of the metamaterial unit cell (1×1 unit cell array structure) in the CST simulator.

GHz to 9.15 GHz) as observed using the RTR method. Meanwhile, for the NRW method, an ENG bandwidth of about 2.46 GHz (6.76-9.22 GHz) and a NZRI bandwidth of about 0.95 GHz (7.80-8.75 GHz) is attained. These results indicate that the proposed MTMs are capable of operating within various frequency bands below 10 GHz, and thus for example, could be applied to new UWB antenna designs to improve performance when considering the aforementioned wearable applications.

II. Proposed Metamaterial Unit Cell Construction

In this work, the proposed material unit cell is simulated considering flexible materials due to its application in a wearable format. For example, conductive and textile-based ShieldIt Super™ from LessEMF Inc. is adopted as the ground plane and the radiators, whereas felt material is employed as its dielectric substrate. Felt has a dielectric constant of 1.44, has a loss tangent of 0.044, and is deemed to be 3 mm thick in our studies. On the other hand, ShieldIt has a conductivity value of 1.18 x 10^5 S/m and a thickness is 0.17 mm. The finite integration technique (FIT) feature in CST Microwave Studio has been utilized to simulate the MTM unit cells and the unit cell array structures.

TABLE I. Parameters Dimensions of the Proposed MTM Unit Cell.

Parameter	Value(mm)	Parameter	Value(mm)
L	6	R4	1.2
W	6	g1	0.5
R1	2.9	g2	0.6
R2	2.2	d	0.5
R3	1.7		

Fig. 1 depicts the step-by-step procedure to design the proposed unit cell, with all dimensional parameters summarized in Table I. Step 1 starts with modelling two decagonal-shaped inner and outer split rings. In step 2, the outer shape has been rotated by 90^0 angle. Followed by the other steps, the unit cell design is completed in step 6.

III. Analysis Methodology

The interaction between the metamaterial structure and the electromagnetic waves displays unique properties. For the metamaterial unit cell which is placed between two waveguide ports on its positive and negative z-axis. To excite the transverse electromagnetic (TEM) wave, a perfect electric conductor (PEC) boundary condition is setup at the x-axis, and a perfect magnetic conductor (PMC) boundary condition at the y-axis, as shown in Fig. 2. A tetrahedral mesh scheme is utilized for the simulation using the frequency solver available in CST. Simulations were performed from 2 to 15 GHz to characterize the metamaterial unit cells. This same setup has been employed for the 2×1 , 1×2 and 2×2 unit cell arrays for their characterization.

The RTR method has been employed to extract the effective parameters from the normal incidences scattering parameters data [10], [21]. The reflection coefficient (S_{11}) and transmission coefficient (S_{21}) are first introduced between the frequency of interest (between 2 and 15 GHz), and their material parameters are then extracted using equations (1) to (7) as follows:

$$S_{11} = \left(\frac{R_{01}(1-e^{i2nk_0d})}{1-R_{01}^{\ 2}e^{i2nk_0d}}\right) \quad (1)$$

$$S_{21} = \left(\frac{(1-R_{01}^{\ 2})e^{ink_0d}}{1-R_{01}^{\ 2}e^{i2nk_0d}}\right) \quad (2)$$

where n is the refractive index, the wave vector in free space denoted as k_0 , the prototype/slab thickness denoted as d and also $R_{01} = \frac{z-1}{z+1}$. Solving equations (1) and (2) results in equation (3), as follows:

$$z = \pm\sqrt{\frac{(1+S_{11})^2 - S_{21}^{\ 2}}{(1-S_{11}^{\ 2}) - S_{21}^{\ 2}}} \quad (3)$$

$$e^{ink_0d} = X \pm i\sqrt{1-X^2} \quad (4)$$

where $X = \frac{1}{2S_{21}(1-S_{11}^{\ 2}+S_{21}^{\ 2})}$

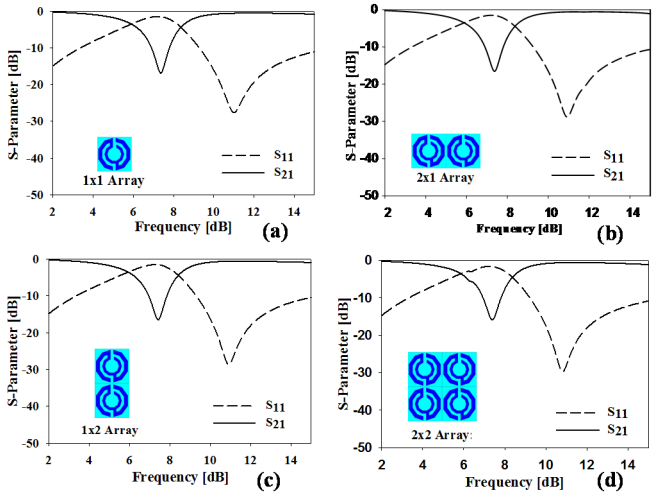

Fig. 3. S-parameters obtained from the different unit cell structures: (a) 1×1 array, (b) 2×1 array, (c) 1×2 array, and (d) 2×2 array.

$$n = \frac{1}{k_0 d}[\{imaginary(\ln e^{ink_0 d}) + 2m\pi\} - i\{real(\ln e^{ink_0 d})\}] \quad (5)$$

where m is an integer value of branch index complexity [23]. Furthermore, the permittivity (ε) and permeability (μ) are expressed as follows equations,

$$\varepsilon = \frac{n}{z} \quad (6)$$

$$\mu = nz \quad (7)$$

The second method in characterizing the material parameters of the MTMs is NRW method [22]. The effective parameters are extracted according to the following equations;

$$V_1 = (S_{21} + S_{11}) \quad (8)$$

$$V_2 = (S_{21} - S_{11}) \quad (9)$$

$$\varepsilon_r \approx \frac{c}{j\pi fd}\frac{1-V_1}{1+V_1} \quad (10)$$

$$\mu_r \approx \frac{c}{j\pi fd}\frac{1-V_2}{1+V_2} \quad (11)$$

TABLE II. RESULTS FOR THE TWO DIFFERENT METHODS

	Permittivity (Real)		NZRI (Real)	
	Array Type	*Bandwidth*	*Array Type*	*Bandwidth*
RTR Method	1×1	2.36 GHz (6.89 -9.25 GHz)	1×1	1.39 GHz (7.76 -9.15GHz)
	2×1	2.36 GHz (6.88-9.24 GHz)	2×1	1.44 GHz (7.76-9.2 GHz)
	1×2	2.34 GHz (6.93-9.27 GHz)	1×2	1.36 GHz (7.84-9.2GHz)
	2×2	2.31 GHz (6.92-9.23 GHz)	2×2	1.34 GHz (7.85-9.18GHz)
NRW Method	1×1	2.51 GHz (6.73-9.24 GHz)	1×1	0.9 GHz (7.75-8.65GHz)
	2×1	2.50 GHz (6.74-9.24 GHz)	2×1	0.98 GHz (7.80-8.78GHz)
	1×2	2.37 GHz (6.25-9.25 GHz)	1×2	0.9 GHz (7.78-8.78GHz)
	2×2	2.46 GHz (6.76-9.22 GHz)	2×2	1 GHz (7.85-8.85GHz)

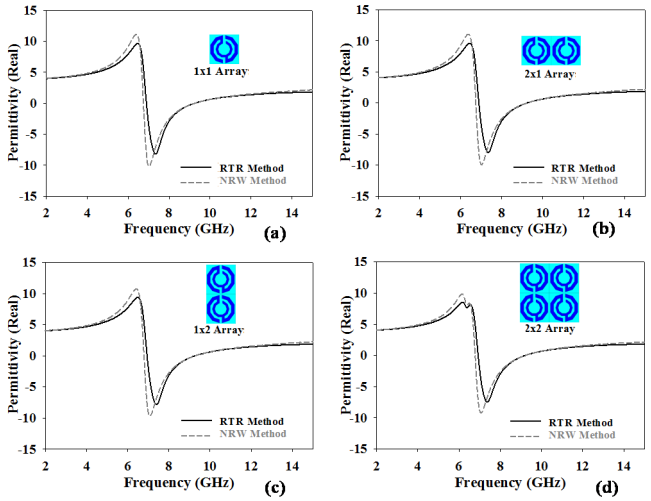

Fig. 4. The real permittivity (ε) values obtained using RTR and NRW methods for different unit cell structures: (a) 1×1 array, (b) 2×1 array, (c) 1×2 array, and (d) 2×2 array.

$$n = \sqrt{\varepsilon_r}\sqrt{\mu_r} \quad (12)$$

where ε_r = effectivity permittivity, μ_r = effectivity permeability, n is the refractive index, d is the thickness of the substrate, and c is the speed of the light.

IV. RESULTS AND DISCUSSION

The simulated scattering parameters of the proposed textile-based material are shown in Fig. 3. Slight discrepancies have been investigated for all of the array conditions in terms of the S_{11} and S_{21} results. The S_{21} has a realized bandwidth of approximately 1 GHz (from 6.8 to 7.8 GHz) for 1×1, 2×1, 1×2 and 2×2 unit cell array structure conditions. Meanwhile, the S_{11} bandwidth is more than 7.1 GHz (from 2 to 3.3 GHz, and from 9.2 to 15 GHz) for all array unit cell structure conditions.

Figs. 4 and 5 shows the permittivity (ε) and NZRI results, respectively for all unit cell structures. Results obtained from the RTR and NRW methods displayed almost similar results regardless of the different magnitude of permittivity and the

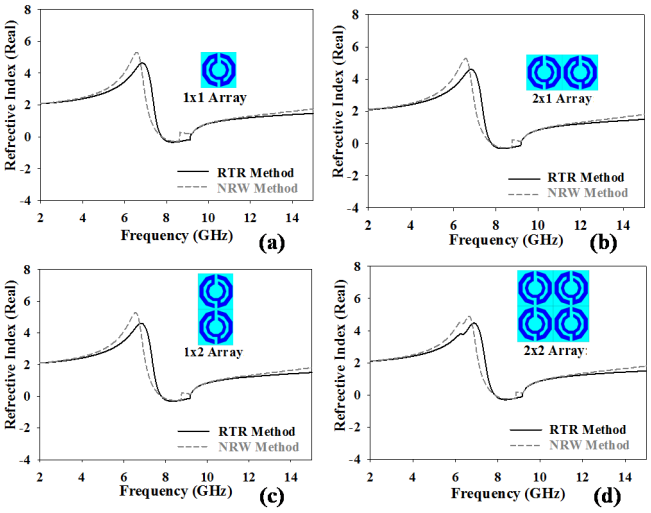

Fig. 5. The real NZRI values obtained using the RTR and NRW methods for different unit cell structures: (a) 1×1 array, (b) 2×1 array, (c) 1×2 array, and (d) 2×2 array.

NZRI value, as summarized in Table II. It is apparent from this table that the NRW method produced a relatively lower refractive index compared to the results obtained from the RTR method. This agrees with the findings reported in [12], which indicates the known ambiguities in extracting refractive index values using the NRW method. Despite the slight variations based on the different extraction methods, values of the ENG and NZRI textile-based unit cells are generally almost identical for all unit cell array structure types. Most importantly, these ENG and NZRI indicates that the structure offers sufficient bandwidth within the UWB band.

V. Conclusion

In this paper, a compact decagonal shaped split ring type metamaterial unit cell based on wearable material has been presented. The investigation to extract effective parameters is developed utilizing two different methods in order to validate the performance of the metamaterial unit cells in the form of 1×1 , 2×1 , 1×2 and 2×2 arrays. Besides that, near-identical results have been observed for the S_{21} and S_{11} for all structures. Regardless of the slight discrepancies in the results obtained from the two different methods, all structures are capable of operating with a minimum ENG bandwidth of 2.35 GHz and about a 1.3 GHz NZRI bandwidth within the UWB band frequency range. Therefore, the proposed wearable and flexible materials can potentially be used to enhance the performance of the UWB antennas and sensors.

Acknowledgment

The author would like to acknowledge the support from the Fundamental Research Grant Scheme (FRGS) under a grant number of FRGS/1/2019/TK04/UNIMAP/02/3 from the Ministry of Education Malaysia

References

[1] A. Chehri and H. T. Mouftah, "Internet of Things - integrated IR-UWB technology for healthcare applications," *Concurr. Comput.* , vol. 32, no. 2, pp. 1–10, 2020.

[2] S. Yan, P. J. Soh, and G. A. E. Vandenbosch, "Wearable ultrawideband technology- A review of ultrawideband antennas, propagation channels, and applications in wireless body area networks," *IEEE Access*, vol. 6, pp. 42177–42185, 2018.

[3] H. Yalduz, B. Koç, L. Kuzu, and M. Turkmen, "An ultra-wide band low-SAR flexible metasurface-enabled antenna for WBAN applications," *Appl. Phys. A Mater. Sci. Process.*, vol. 125, no. 9, pp. 1–11, 2019.

[4] G. Gao, B. Hu, S. Wang, and C. Yang, "Wearable planar inverted-F antenna with stable characteristic and low specific absorption rate," *Microw. Opt. Technol. Lett.*, vol. 60, no. 4, pp. 876–882, 2018.

[5] A. Iqbal, A. Smida, A. J. Alazemi, M. I. Waly, N. Khaddaj Mallat, and S. Kim, "Wideband Circularly Polarized MIMO Antenna for High Data Wearable Biotelemetric Devices," *IEEE Access*, vol. 8, pp. 17935–17944, 2020.

[6] P. B. Samal, P. J. Soh, H. Xu, and G. A. E. Vandenbosch, "Microstrip-based all-textile unidirectional UWB antenna with full ground plane," *8th Eur. Conf. Antennas Propagation, EuCAP 2014*, no. EuCAP, pp. 1408–1412, 2014.

[7] G. P. Gao, B. Hu, S. F. Wang, and C. Yang, "Wearable Circular Ring Slot Antenna with EBG Structure for Wireless Body Area Network," *IEEE Antennas Wirel. Propag. Lett.*, vol. 17, no. 3, pp. 434–437, 2018.

[8] A. Alemaryeen and S. Noghanian, "Crumpling effects and specific absorption rates of flexible AMC integrated antennas," *IET Microwaves, Antennas Propag.*, vol. 12, no. 4, pp. 627–635, 2018.

[9] S. Ahdi Rezaeieh, M. A. Antoniades, and A. M. Abbosh, "Gain Enhancement of Wideband Metamaterial-Loaded Loop Antenna with Tightly Coupled Arc-Shaped Directors," *IEEE Trans. Antennas Propag.*, vol. 65, no. 4, pp. 2090–2095, 2017.

[10] Al-Bawri *et al.*, "Compact Ultra-Wideband Monopole Antenna Loaded with Metamaterial," *Sensors*, vol. 20, no. 3, p. 796, Jan. 2020.

[11] M. K. Khandelwal, A. Arora, S. Kumar, K. W. Kim, and H. C. Choi, "Dual band double negative (DNG) metamaterial with small frequency ratio," *J. Electromagn. Waves Appl.*, vol. 32, no. 17, pp. 2167–2181, 2018.

[12] H. Singh, B. S. Sohi, and A. Gupta, "A compact CRLH metamaterial with wide band negative index characteristics," *Bull. Mater. Sci.*, vol. 42, no. 4, pp. 1–11, 2019.

[13] S. Zahertar, Y. Wang, R. Tao, J. Xie, Y. Q. Fu, and H. Torun, "A fully integrated biosensing platform combining acoustofluidics and electromagnetic metamaterials," *J. Phys. D. Appl. Phys.*, vol. 52, no. 48, 2019.

[14] M. Naserpour, C. J. Zapata-Rodríguez, S. M. Vuković, H. Pashaeiadl, and M. R. Belić, "Tunable invisibility cloaking by using isolated graphene-coated nanowires and dimers," *Sci. Rep.*, vol. 7, no. 1, pp. 1–14, 2017.

[15] A. Presse and A. C. Tarot, "Miniaturized bendable 400 MHz artificial magnetic conductor," *Appl. Phys. A Mater. Sci. Process.*, vol. 122, no. 4, pp. 1–5, 2016.

[16] A. K. Panda, M. Pattnaik, and R. Swain, "CSRR Embedded CPW Band-Stop Filter," *IETE J. Res.*, vol. 0, no. 0, pp. 1–7, 2019.

[17] A. Salim and S. Lim, "Review of recent metamaterial microfluidic sensors," *Sensors (Switzerland)*, vol. 18, no. 1, 2018.

[18] A. X. Wang, S. B. Qu, H. L. Dai, G. P. Zhang, W. J. Wang, and M. B. Yan, "Design of Ultrathin Five-band Polarization Insensitive Metamaterial Absorbers," *Proc. 2019 IEEE 2nd Int. Conf. Electron. Inf. Commun. Technol. ICEICT 2019*, pp. 658–661, 2019.

[19] S. S. Islam, M. R. Iqbal Faruque, and M. T. Islam, "Design and absorption analysis of a new multiband split-S-shaped metamaterial," *Sci. Eng. Compos. Mater.*, vol. 24, no. 1, pp. 139–148, 2017.

[20] M. M. T. Islam, M. M. T. Islam, M. Samsuzzaman, and M. R. I. Faruque, "Compact metamaterial antenna for UWB applications," *Electron. Lett.*, vol. 51, no. 16, pp. 1222–1224, 2015.

[21] X. Chen, T. M. Grzegorczyk, B. I. Wu, J. Pacheco, and J. A. Kong, "Robust method to retrieve the constitutive effective parameters of metamaterials," *Phys. Rev. E - Stat. Physics, Plasmas, Fluids, Relat. Interdiscip. Top.*, vol. 70, no. 1, p. 7, 2004.

[22] M. M. Hasan, M. R. I. Faruque, S. S. Islam, and M. T. Islam, "A new compact double-negative miniaturized metamaterial for wideband operation," *Materials (Basel).*, vol. 9, no. 10, pp. 1–12, 2016.

[23] S. S. Islam, M. R. I. Faruque, and M. T. Islam, "A new direct retrieval method of refractive index for the metamaterial," *Curr. Sci.*, vol. 109, no. 2, pp. 337–342, 2015.